Ultrahigh-Accuracy Body-Pointing System for the Large Space Telescope

S. Calvin Rybak,* Ronald A. Mayo,† Stanley I. Lieberman,‡ and Larry L. Hartter§
The Bendix Corporation, Southfield, Mich.

The purpose of the Large Space Telescope (LST) program is to place a 3-m diffraction-limited telescope in a 270-n.mi. orbit to perform astronomical observations that are not presently possible with Earth-bound telescopes. Pointing stability requirements necessary to assure diffraction-limited images are ±0.005 arc-sec, over possible experiment observation times of several hours. In order to determine whether these stringent pointing requirements could be met, a complex simulation model was defined which consisted of detailed dynamic representations of control moment gyros (CMG's) and reaction wheels (RW's), including their noise characteristics, dynamic sensor representations with sensor noise, shock mounts for the CMG actuators, a detailed representation of an image motion compensation (IMC) system, and a detailed flexible body structural model with all significant vehicle and solar panel bending modes. On the basis of both stability and performance studies utilizing this model, it was determined that a body-pointing system will meet LST requirements in the presence of CMG vibrational disturbances and sensor noise. The recommended system consists of three orthogonally mounted RW's for primary short-term control, and a cluster of CMG actuators for continuous RW desaturation and vehicle maneuvering. This system has several levels of redundancy, including the possibility of achieving pointing stability requirements with the CMG system alone.

Introduction

TO meet the goal of diffraction-limited images, the Large Space Telescope (LST) will require pointing stability on the order of 2.43×10^{-8} rad (0.005 arc-sec) over experimental observation times that can last for hours. Two control philosophies that can be adopted to meet these stringent requirements are the following:

1) Image motion compensation (IMC): Stabilize the total vehicle to accuracies in the range of 4.85×10^{-7} to 4.85×10^{-6} rad (0.1 to 1.0 arc-sec) by means of a control moment gyro (CMG) base stabilization system, and employ a vernier control system internal to the telescope to stabilize the image to the required accuracy of 2.43×10^{-8} rad (0.005 arc-sec).

2) Body point: stabilize the total vehicle to the desired accuracy of 2.43×10^{-8} rad (0.005 arc-sec).

Initial feasibility of a body-pointing system meeting LST pointing stability requirements was demonstrated in Ref. 1. It was demonstrated that a body-pointing system consisting of large CMG's (678 N-m-sec momentum capacity) with small reaction wheels (RW's) (2 N-m output torque; 2 N-m-sec momentum capacity) could achieve the required LST accuracies. However, simplified simulation models were used in that initial analysis for the sensors (position and rate), actuators (CMG's and RW's), and vehicle structure.

A subsequent study was conducted and reported in Ref. 2. The primary purpose of that study was to eliminate the simplifications of the initial feasibility study and determine the performance capability of a body-pointing system using CMG's alone, and CMG's augmented by small RW's. Other objectives of the study were to 1) investigate the effects of solar panel flexibility on pointing performance and determine whether a "stiff" or "soft" panel design should be employed, 2) determine the sensor implementation yielding optimum pointing performance in the presence of sensor and actuator noise, and 3) define the magnetic moment control law and system implementation for a magnetic moment desaturation system. Although this study included the dynamic effects of mounting the CMG's on 20-Hz shock mounts, the pointing errors incurred from CMG vibrational disturbances were not investigated. In addition, the CMG gimbal friction was modeled in a classical manner exhibiting stiction, breakout, and running frictional characteristics. During stiction, relative motion between the CMG gimbal and its base was assumed to be zero. More recent analyses and testing[3] indicate that relative motion between the CMG gimbal and its base always exists, even when the CMG is in the so-called "stiction" region. When in stiction, a compliant characteristic is exhibited similar to the stress-strain relationship that characterizes most materials. In this context, "breakout" can be considered as the fracture point of this elastic characteristic. Therefore, the objectives of the present study are to: 1) update the CMG gimbal frictional characteristics to a compliant model and re-examine the pointing performance that can be achieved via body pointing for systems employing CMG's only and CMG's with RW's. 2) investigate the pointing errors incurred due to CMG vibrational disturbances for hard-mounted and shock-mounted conditions, and 3) investigate the performance of an IMC system using secondary mirror articulation. The performances achieved by the IMC and body-pointing systems are compared, and a recommendation for the LST stabilization system configuration is made.

The basic conclusion of all studies performed to date is that LST image stability can be achieved by body pointing with a combined CMG/RW system. With a compliant frictional representation for CMG gimbal friction, required LST pointing performance also can be obtained using the CMG's alone. In addition, projected CMG vibrational disturbances require that they be shock-mounted. A 20-Hz passive shock mount will reduce the pointing errors incurred by vibrations to acceptable levels. A summary of the analyses performed and the results obtained during the present study are presented in the following paragraphs.

Received April 9, 1975; revision received Nov. 10, 1975. This work was supported by NASA Marshall Space Flight Center under Contracts NAS8-28983 and NAS8-29152.

Index category: Spacecraft Attitude Dynamics and Control.

*Head, Guidance and Control, Energy, Environmental and Technology Office, Denver, Colo.

†Project Engineer, Guidance Systems Division, Denver, Colo.

‡Director, Information Processing Department, Research Laboratories. Member AIAA.

§Project Engineer, Mechanical Engineering Department, Research Laboratories.

Model Description

A coupled flexible body vehicle model with all significant bending modes, including those due to the solar panels, was represented. First-order position sensor dynamics and second-order rate gyro dynamics were defined. Sensor noise characteristics were represented by white noise, bandlimited at 50 Hz.

The simulation was performed with a pyramid arrangement of four single-gimbal CMG's. The dynamics of each CMG initially included the effects of gimbal compliance, cogging and ripple torques, and gimbal frictional chracteristics. Subsequent study, however, indicated that cogging and ripple had negligible effect on CMG performance and thus were eliminated. In addition, each CMG was mounted on a 20-Hz shock mount to isolate the vehicle from CMG vibrational disturbances due to wheel imbalances and principal axis misalignments. Second-order shock mount dynamics were assumed. CMG torque noise, represented as tachometer noise, which is its prime source, also was included in the simulation and modeled as 50-Hz bandlimited white noise.

The RW dynamics included the primary torque noise sources due to cogging and ripple, coulomb friction, magnetic drag, torque motoamics, and saturation. RW friction was modeled only as coulomb friction, since the RW's were run in a biased state. This was feasible because of their small momentum requirements. Hence, the RW's would exhibit only coulomb friction, and the frictional characteristics around zero are unimportant. RW vibration disturbances were assumed negligible because of the small size and mass of the wheels and were not included in the simulation. RW tachometer noise was represented as 50-Hz bandlimited white noise.

The IMC system model included coupling between the secondary mirror articulation system and vehicle flexibility, and a complete description of the dynamic interaction between the IMC system and the CMG base stabilization system. The analog-to-digital (A/D) and digital-to-analog (D/A) interfaces were simulated as they would occur in the onboard system. These interfaces included the effects of sampling and quantization. The sampling frequency was chosen to yield satisfactory system response without the addition of compensation. The quantization level was chosen by examining the peak sensor and actuator commands due to peak disturbances. These levels then were increased one order of magnitude, and the resultant level was quantized using 14-bit A/D and D/A convertors.

The environmental effects consisted of gravity gradient torques. The vehicle coordinate system is shown in Fig. 1. The 0.005-arc-sec pointing requirement applies to the vehicle Y and Z axes only. The requirement for the X axis is 0.1 arc-sec.

A flexible body nodal diagram of the vehicle is shown in Fig. 2. Figures 3 and 4 are block diagrams of the complete hybrid simulation model. The CMG actuator dynamics are illustrated in Fig. 5, and the RW dynamics in Fig. 6. Figure 7 is a representation of the mirror articulation system, including coupling with vehicle flexibility.

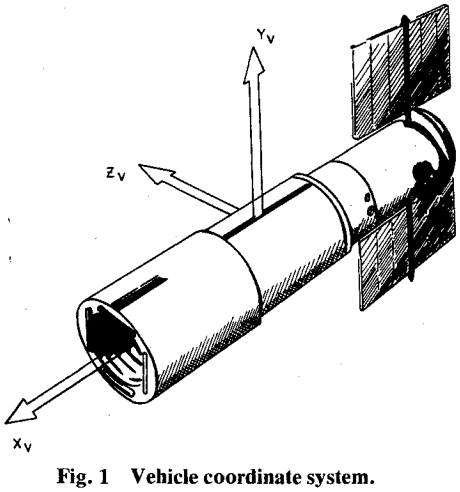

Fig. 1 Vehicle coordinate system.

Vehicle Control Law and Stability

The vehicle attitude control law consists of an algebraic summation of error quantities proportional to vehicle rate, position, and the integral of position. The integral of position error eliminates the angular hangoff that otherwise would occur because of gravity gradient disturbances. The rate, position, and integral gains yielding particular vehicle loop bandwidths were calculated based on rigid body dynamics. The gains then were programmed into the complex hybrid simulation model, and vehicle stability margins were investigated for a range of loop bandwidths between 0.4 and 5 Hz. Adequate margins were maintained for all loop bandwidths for the CMG/RW system. The CMG system, however, exhibited marginal stability characteristics for vehicle bandwidths in excess of 3 Hz.

Because of uncertainties in determining vehicle bending modes, stability for the CMG, CMG/RW, and IMC systems also was investigated as a function of bending mode variations. The quantities, natural frequency and damping, were varied by modifying separately all of the modal frequencies and damping ratios a fixed percentage from the nominal values given in the NASA-furnished modal data. Vehicle stability was determined by establishing rate and position gain margins as functions of loop bandwidth, with bending mode variation as a parameter. The results for the CMG and CMG/RW systems indicate that vehicle stability is affected severely when the bending mode natural frequencies are decreased by 50% from nominal. Should such variations occur, additional compensation would be required if vehicle loop bandwidths in excess of 1 Hz were desired. Decreasing modal damping by 66% also decreased stability for both the CMG and CMG/RW systems, particularly in the 2- to 5-Hz bandwidth range. However, for both the CMG and CMG/RW systems, adequate stability margins still are obtained for vehicle loop bandwidths of 3 Hz or less, without any additional compensation.

For the IMC system, attitude loop stability is affected somewhat by bending mode variations, but IMC loop stability apparently is independent of both a 50% decrease in modal frequency and a 66% decrease in damping ratio. Overall, the IMC system yielded better stability characteristics in the presence of bending mode variations than either the CMG or CMG/RW systems. These results were obtained without the use of a counterbalance mechanism to eliminate the disturbances applied to the vehicle due to secondary mirror activation. Further study is required to determine whether an IMC system without counterbalancing is inherently less sensitive to bending mode parameter variations than an equivalent body-point system, as the results of this study apparently indicate. However, it should be noted that an IMC system potentially can be made less sensitive to bending mode variations by the use of counterbalancing. This is apparent, for, if counterbalancing were achieved perfectly, the IMC system would be isolated completely from the vehicle, and its operating characteristics would be independent of vehicle dynamic description.

Effects of CMG Nonlinearities

The prime nonlinearity associated with a CMG is its gimbal frictional characteristics. When CMG gimbal friction is modeled in a classical manner (with stiction, breakout, and running friction), limit cycles occur in a disturbance-free environment over a wide range of vehicle bandwidths.[2] The pointing accuracy achieved by a CMG system using nominal stiction and running friction values of 0.37 and 0.29 N-m, respectively, was between 2.43×10^{-9} and 4.85×10^{-9} rad (0.0005 to 0.001 arc-sec) for vehicle bandwidths ranging be-

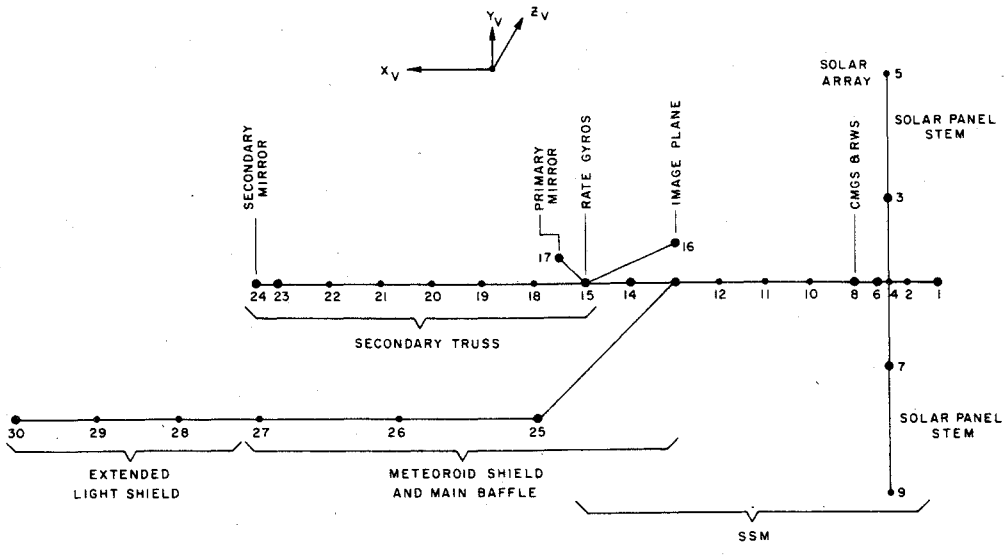

Fig. 2 Flexible body nodal diagram.

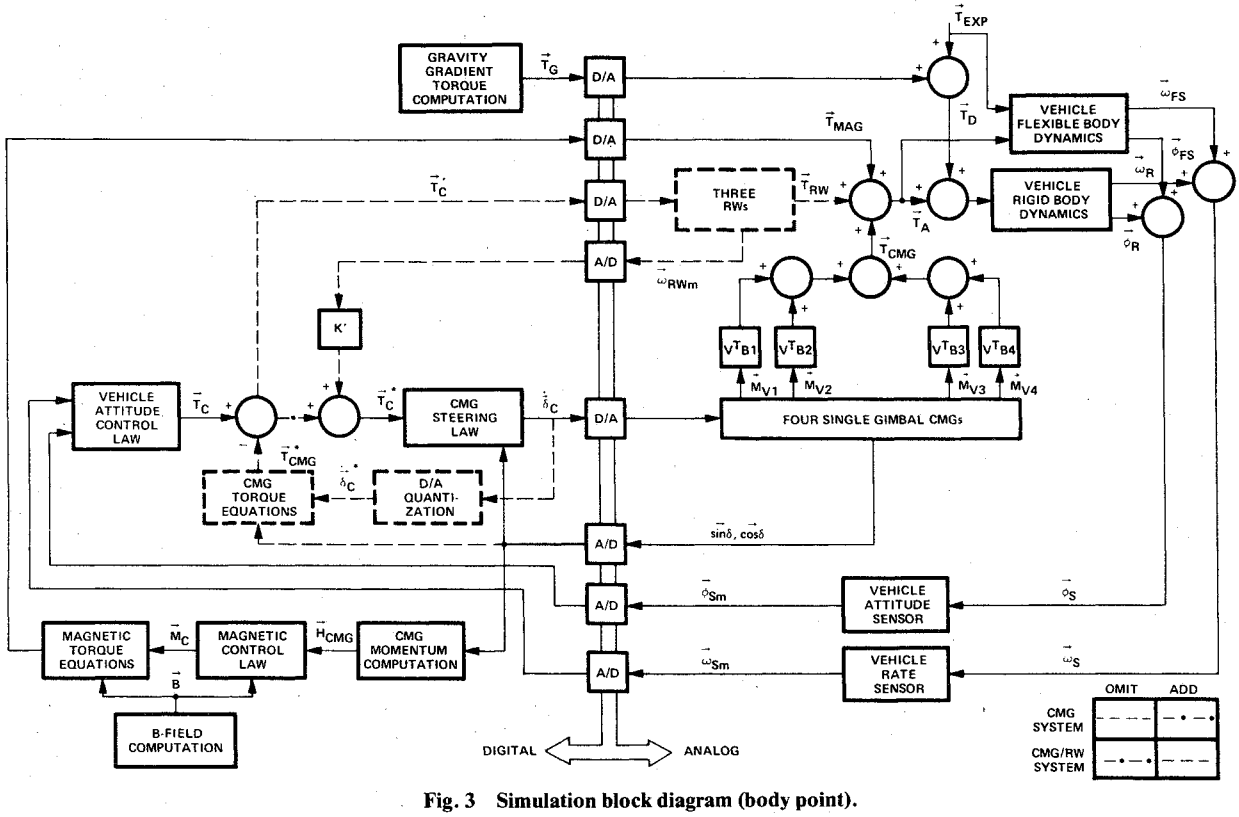

Fig. 3 Simulation block diagram (body point).

tween 1 and 3 Hz. The pointing accuracy achieved by the CMG/RW system was approximately one order of magnitude better than that obtained by the CMG system over the same bandwidth range. In the present study, the CMG gimbal friction model used reflects some of the more current analyses and testing[3] of the friction phenomenon.

CMG gimbal friction, illustrated in Fig. 8, indicates that a compliance characteristic is exhibited during stiction, analogous to the stress-strain characteristics of many materials. Running friction then can be considered to be the frictional value at which fracture of the frictional bond occurs. The frictional characteristics shown in Fig. 8 closely approximate test data that were obtained on LST-type CMG's,[4] and hence can be used as relatively simple representations of friction in both analysis and simulation. When these frictional characteristics are employed, vehicle limit cycles do not occur for a CMG system under disturbance-free conditions over a wide range of system bandwidths, frictional spring constants (10,000 to 50,000 N-m/rad), and running friction levels (0.1 to 0.5 N-m). Therefore, the pointing accuracies obtained from both the CMG and CMG/RW systems are equivalent. When the vehicle is disturbed, the pointing accuracies achieved by the CMG and CMG/RW systems also are equivalent, and less than 0.0001 arc-sec, regardless of whether a classical or compliant representation of gimbal friction is employed.[2] Based upon these results, the small RW's can be eliminated without incurring a performance penalty, thus reducing the cost and complexity of the body-point system. However, it should be emphasized that the results obtained are dependent on the functional representation of gimbal friction. If the actual CMG gimbal friction is significantly different from that used in this study, vehicle limit cycles are possible, and a significant improvement in performance would be realized by the addition of small RW's. However, at a very minimum, CMG's would offer an excellent backup to a CMG/RW system. Future study of CMG gimbal frictional chracteristics and

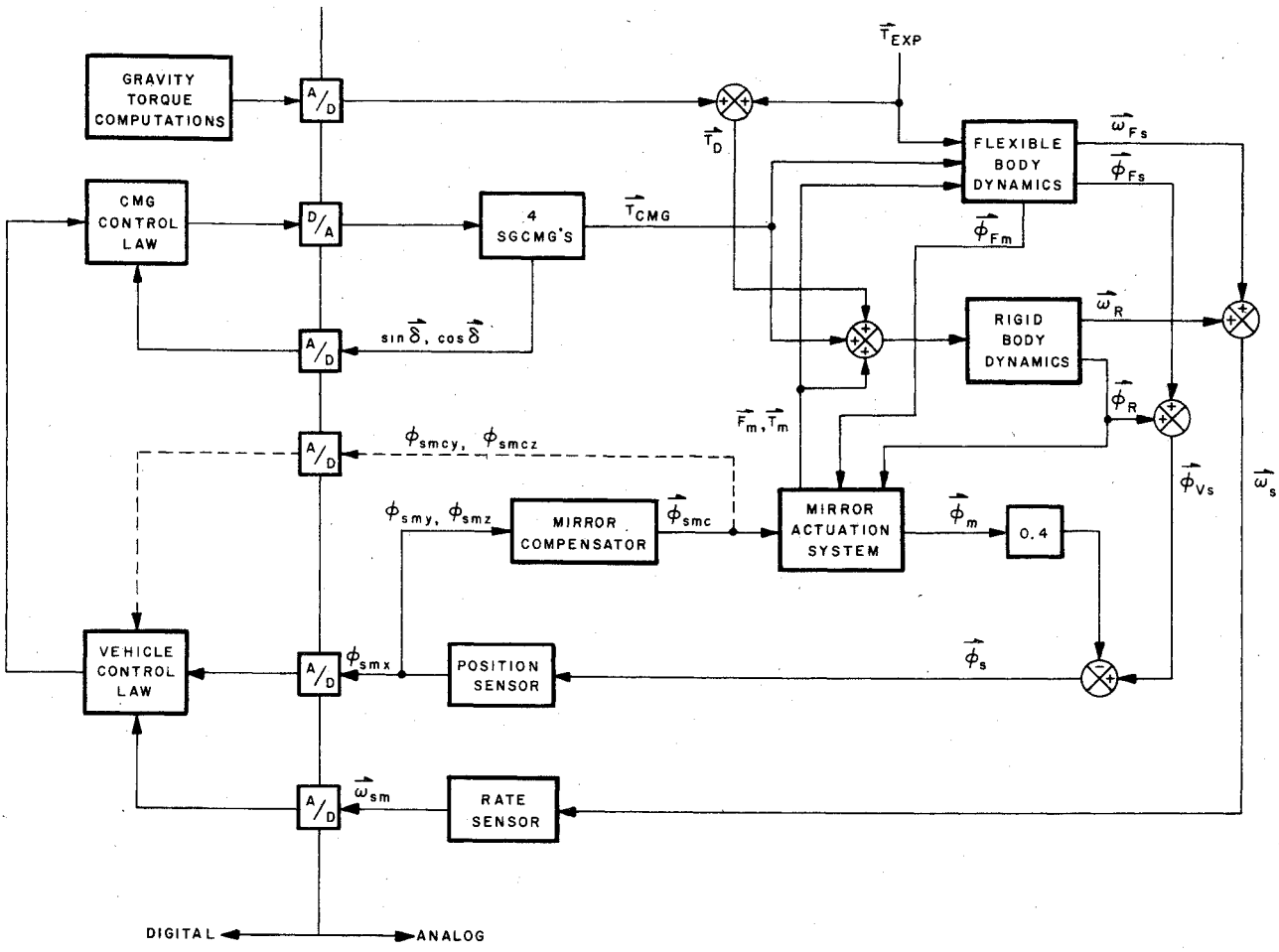

Fig. 4 Simulation block diagram (IMC).

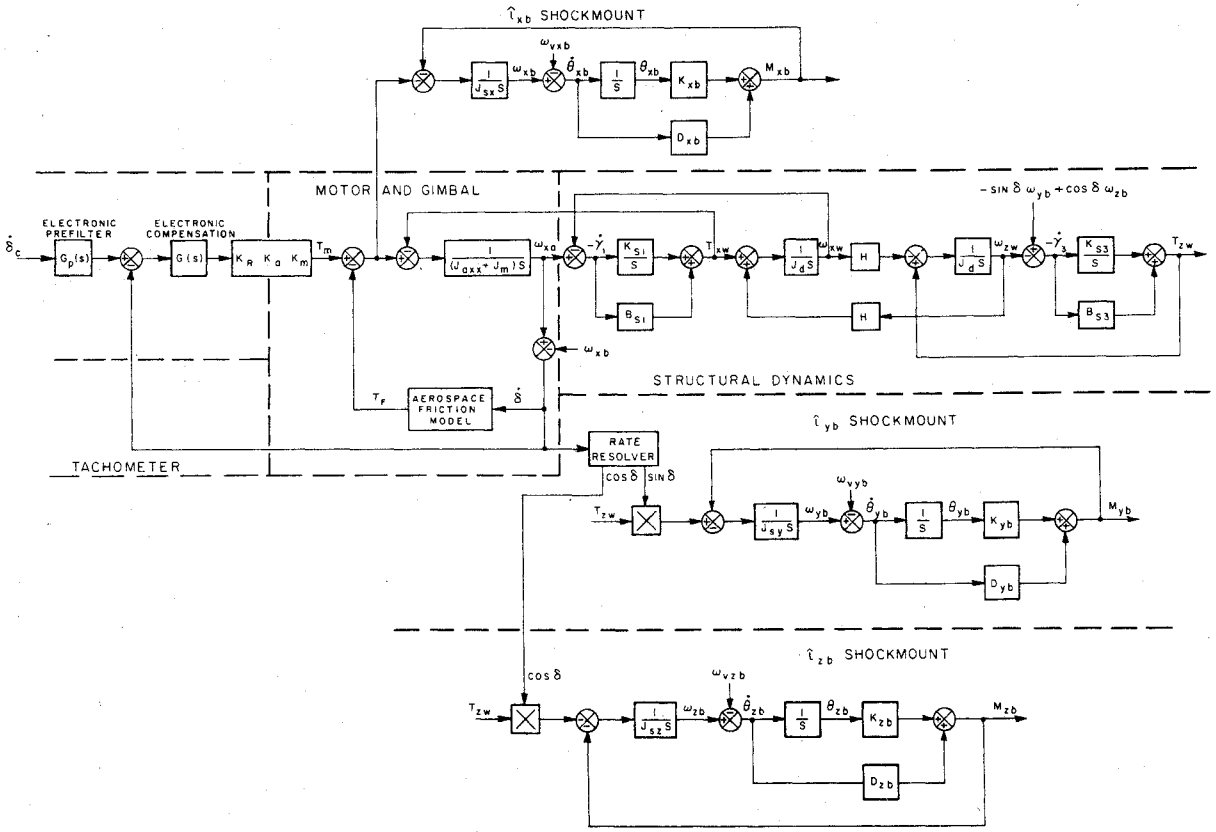

Fig. 5 CMG servo model.

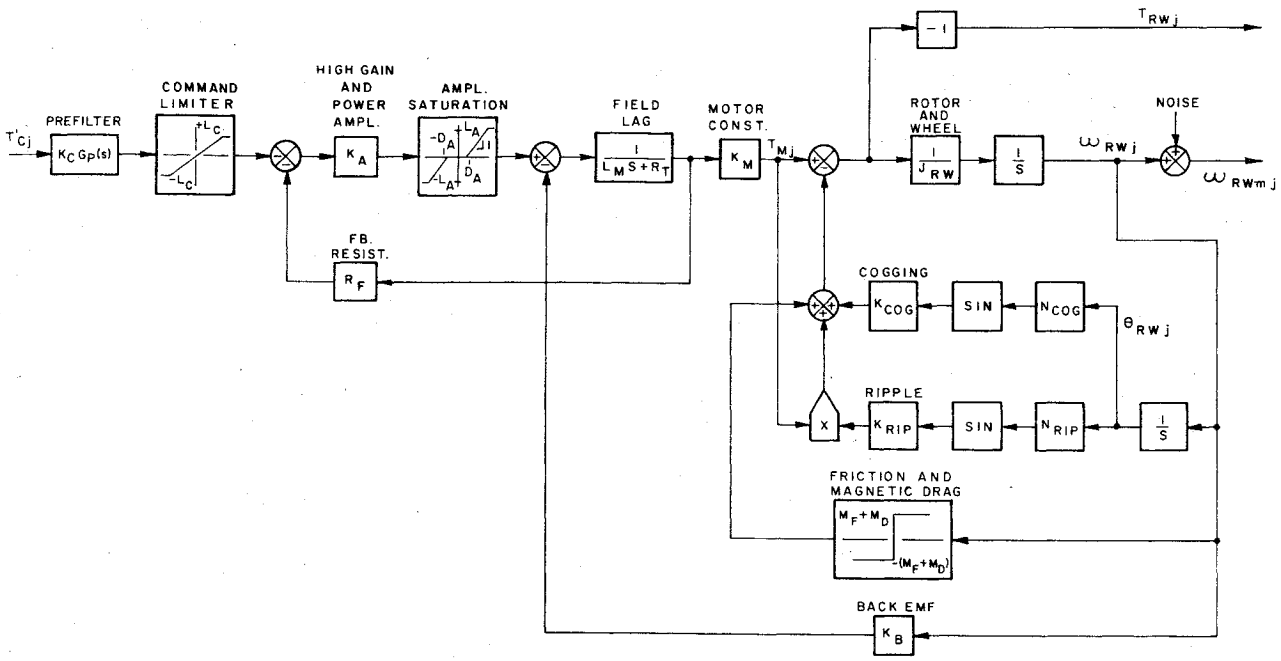

Fig. 6 RW model.

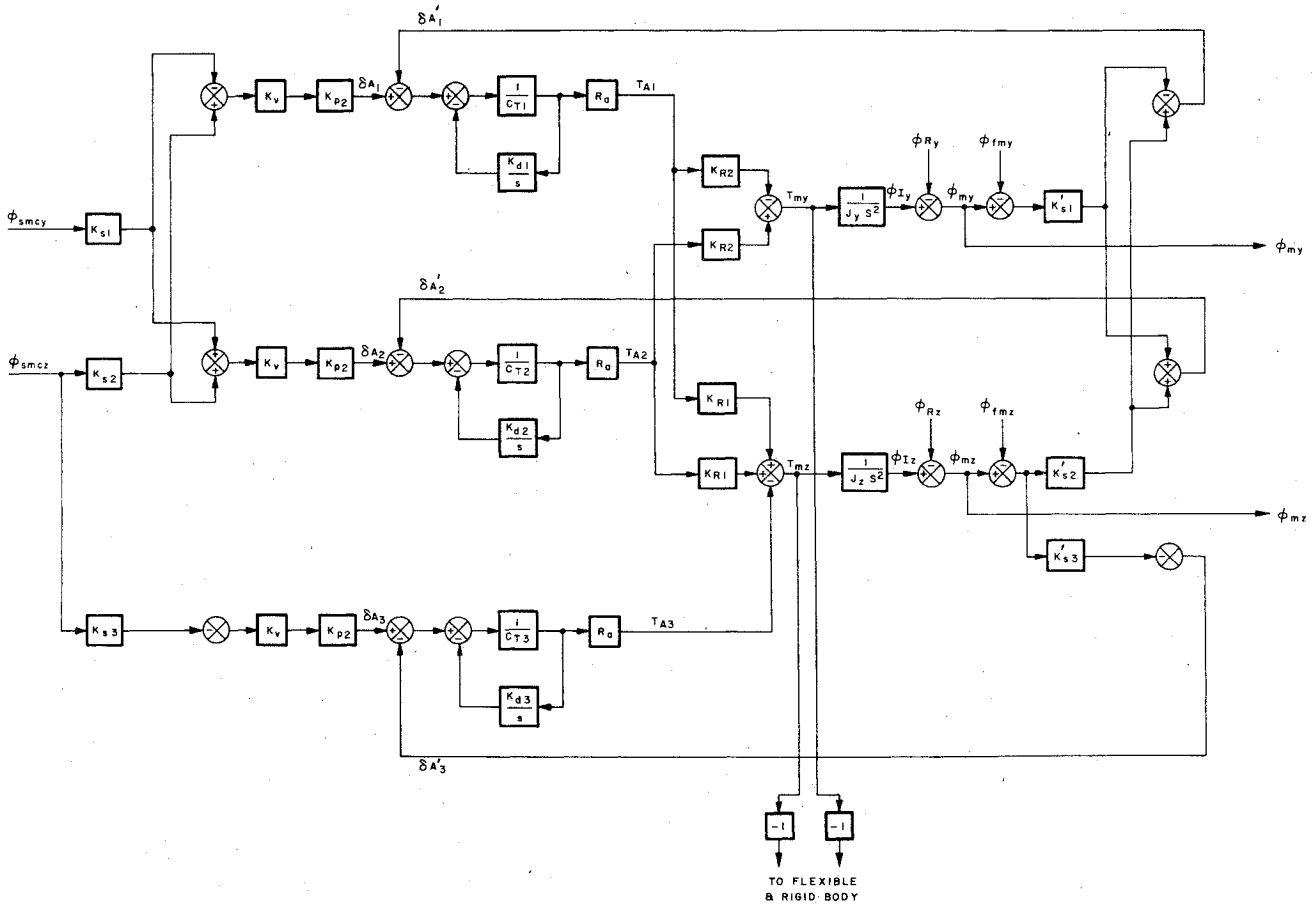

Fig. 7 Secondary mirror articulation system.

their variations over time will establish with a greater degree of confidence whether RW's can be eliminated altogether.

System Noise Studies

It has been established[2] that it will be necessary to operate the control system at relatively high bandwidths (i.e., near 2 Hz) in order to control solar panel disturbances. However, as loop bandwidth increases, the errors due to various noise sources usually increase. These errors can become excessive until vehicle pointing requirements are not met. Therefore, several noise studies were performed for both body-point and IMC systems. These studies included an investigation of the effects of position sensor noise, rate gyro noise, CMG tachometer noise, and RW tachometer noise. In order to determine the sensor configuration that would achieve optimum pointing performance for a body-point system in the presence of noise, pointing errors were specified for three sen-

sor implementations: rate-plus-position, derived rate, and rate gyro hold.

For the IMC system, two sensor configurations were investigated: rate-plus-position and derived rate. Rate gyro hold has no meaning when considering an IMC system. All noise sources were modeled by 50-Hz bandlimited white noise in the absence of any other definitive data at the time of study performance. However, these results can be used to specify sensors and actuators in terms of noise equivalent angle, rate, and torque requirements by integrating the amplitude of the flat power spectral density over the control loop bandwidth. The results obtained in this manner are largely independent of the actual shape of the individual power spectral densities. The following paragraphs summarize these studies.

For both body-point (CMG, CMG/RW) and IMC systems, vehicle pointing errors for an individual noise source did not always increase with increasing loop bandwidth. For example, in all sensor implementations considered, pointing errors increased with increasing loop bandwidth for position noise, and decreased for CMG tachometer noise. Therefore, it is reasonable to expect that a particular loop bandwidth will yield optimum vehicle pointing performance from system noise considerations alone. This bandwidth will vary as a function of the relative levels between the individual noise sources. The nominal amplitudes for the noise sources considered in this study were chosen such that each individual source would result in approximately 0.001 arc-sec rms pointing error at a loop bandwidth of 2 Hz for a body-point system. This criterion resulted in the following noise power spectral density amplitudes

$$\text{position sensor noise} = 2.35\times10^{-18}\ \frac{\text{rad}^2}{\text{Hz}}\ \left[1\times10^{-7}\ \frac{\text{arc-sec}^2}{\text{Hz}}\right]$$

$$\text{rate gyro noise} = 1.88\times10^{-16}\ \frac{(\text{rad/sec})^2}{\text{Hz}}\ \left[8\times10^{-6}\ \frac{(\text{arc-sec/sec})^2}{\text{Hz}}\right]$$

$$\text{CMG tachometer noise} = 2\times10^{-10}\ \frac{(\text{rad/sec})^2}{\text{Hz}}\ \left[6.6\times10^{-7}\ \frac{(\text{deg/sec})^2}{\text{Hz}}\right]$$

$$\text{RW tachometer noise} = 1\times10^{-2}\ \frac{(\text{rad/sec})^2}{\text{Hz}}\ \left[32.8\ \frac{(\text{deg/sec})^2}{\text{Hz}}\right]$$

Overall system pointing performance, when all noise sources are operating simultaneously, can be derived by root sum squaring (rss) the effects of individual noise sources, since all of the noise sources considered are independent and uncorrelated.

Figure 9 shows total CMG system performance as a function of vehicle loop bandwidth using a rate-plus-position sensor implementation. In this implementation, position is derived from telescope optics, whereas rate information is obtained independently from rate gyros. Figures 10 and 11 show similar data for derived rate and rate gyro hold sensor implementations, respectively. For derived rate, the rate signals are obtained by differentiating the telescope derived position signals; for rate gyro hold, position is derived by integrating the rate gyro signals. Only the Y-axis errors are illustrated in the figures. The Z-axis errors are approximately equal to the Y-axis errors. The preceding curves used nominal values for the various noise sources, except for the derived rate system, which used a position noise source one-fourth nominal.

Examination of the curves shows that, for nominal noise values, CMG system pointing performance is essentially equivalent for rate-plus-position and rate gyro hold sensor implementations. For the rate-plus-position sensor implementation, minimum pointing errors occurred at a vehicle loop bandwidth of 2 Hz. With the derived rate sensor implementation, where the system is more sensitive to position noise than with the rate-plus-position sensor implementation, the loop bandwidth at which minimum pointing errors occurred was lowered to 1 Hz. For rate gyro hold, the vehicle loop bandwidth at which minimum pointing errors occurred was 3 Hz. The minimum vehicle X, Y, and Z axes rss pointing errors for the three sensor implementations are summarized in Table 1 and indicate acceptable pointing accuracies for all three sensor implementations for the given noise levels.

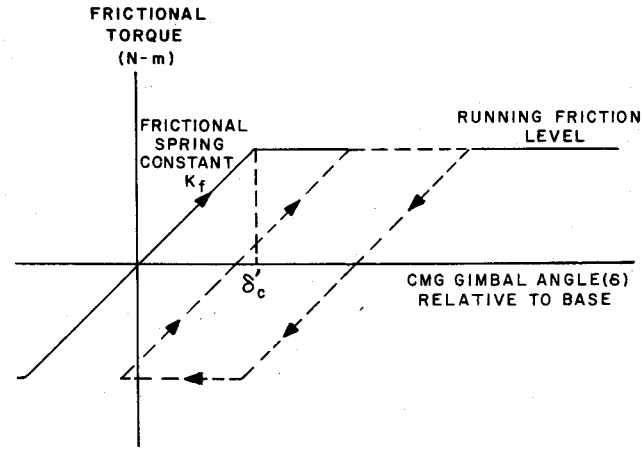

Fig. 8 CMG gimbal friction.

CMG/RW system pointing errors about the Y and Z axes, for all sensor implementations considered, are approximately equal to the pointing errors obtained with the CMG system. Again, best pointing performance is obtained for the rate-plus-position sensor implementation for the nominal noise values. Minimum pointing errors, and the loop bandwidths at which they occur, are listed in Table 1.

IMC System Performance

The IMC system achieves high pointing accuracy through articulation of the telescope secondary mirror. The total vehicle is stabilized by a base stabilization system (CMG system) to an accuracy of approximately 4.85×10^{-7} rad (0.1 arc-sec), with the added degree of stability needed to meet LST image stability requirements of 2.42×10^{-8} rad (0.005 arc-sec) obtained by the IMC system through secondary mirror articulation. Adequate X-axis pointing stability, which is unaffected by this mirror articulation, is maintained by the base stabilization system. The bandwidth of the CMG base stabilization system is one order of magnitude below that of the IMC system, thereby minimizing the interaction between the two. The position error signal that drives the IMC system is identical to that which drives the body point system and is derived from the telescope optics. The position error signal that drives the CMG system is proportional to secondary mirror angular displacement relative to the vehicle and is obtained from the output of the IMC system compensation network. The sensor implementations that were investigated for the IMC system were rate-plus-position and derived rate. For the rate-plus-position implementation, rate signals required by the CMG system are generated by rate gyros, whereas for

Table 1 Summary of system pointing performance

System	Rate-plus-position				Derived rate[a]				Rate gyro hold			
	Freq., Hz.	X-axis pointing error	Y-axis pointing error	Z-axis pointing error	Freq., Hz	X-axis pointing error	Y-axis pointing error	Z-axis pointing error	Freq., Hz.	X-axis pointing error	Y-axis pointing error	Z-axis pointing error
CMG system	2.0	1.935×10^{-8} rad 0.004 arc-sec	8.25×10^{-9} rad 0.0017 arc-sec	9.22×10^{-9} rad 0.0019 arc-sec	1.0	2.91×10^{-8} rad 0.006 arc-sec	1.07×10^{-8} rad 0.002 arc-sec	1×10^{-8} rad 0.0022 arc-sec	3.0	1.21×10^{-8} rad 0.0025 arc-sec	9×10^{-9} rad 0.00185 arc-sec	8×10^{-9} rad 0.00165 arc-sec
CMG/RW system	2.0	2.08×10^{-8} rad 0.0043 arc-sec	8.96×10^{-9} rad 0.00185 arc-sec	9.45×10^{-9} rad 0.00195 arc-sec	1.25	3.15×10^{-8} rad 0.0065 arc-sec	9.45×10^{-9} rad 0.00195 arc-sec	9.7×10^{-9} rad 0.002 arc-sec	2.5	1.7×10^{-8} rad 0.0035 arc-sec	9.22×10^{-9} rad 0.0019 arc-sec	8.75×10^{-9} rad 0.0018 arc-sec
IMC system	1.75	2.42×10^{-8} rad 0.005 arc-sec	1.21×10^{-8} rad 0.0025 arc-sec	1.21×10^{-8} rad 0.0025 arc-sec	1.25[b]	1.455×10^{-8} rad 0.003 arc-sec	5.34×10^{-9} rad 0.0011 arc-sec	5.34×10^{-9} rad 0.0011 arc-sec	Not applicable			

[a] Position noise power spectral density at one-fourth nominal for derived rate system.
[b] CMG tachometer noise power spectral density one-tenth nominal for IMC system derived rate sensor implementation.

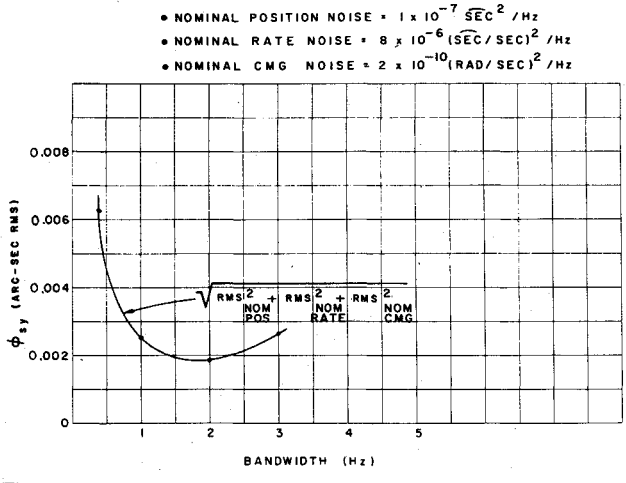

Fig. 9 Y-axis total rms pointing error resulting from noise sources: CMG system.

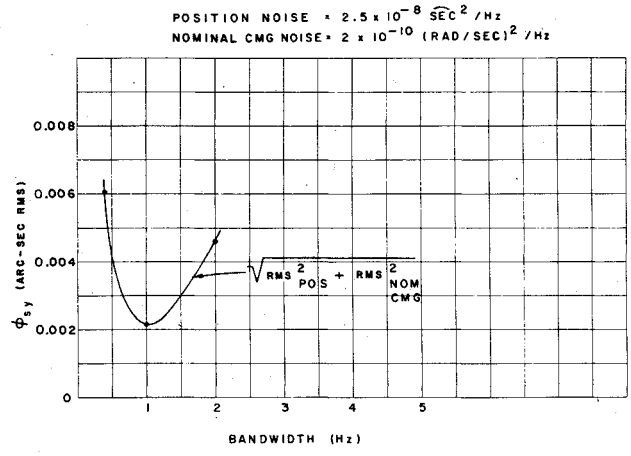

Fig. 10 Y-axis total rms pointing error resulting from noise sources: derived rate control, CMG system.

the derived rate implementation, the rate signals are obtained by differentiation of the position signals obtained from the IMC compensator networks. A rate gyro hold sensor implementation has no real application in an IMC system, since the telescope-generated position signal still is required to drive the IMC system, and hence its noise contribution still is present. The pointing accuracy achieved by the IMC system was virtually identical for the Y and Z axes. Thus, results will be shown for the Y axis only.

Figure 12 illustrates the image stability achieved by the IMC system for the rate-plus-position sensor implementation with nominal values of all noise sources. The vehicle bandwidth for which minimum errors are obtained for the vehicle Y and Z axes is 2.0 Hz. At this bandwidth, the rms pointing accuracies achieved were 2.42×10^{-8} rad (0.005 arc-sec) about the X axis, and 1.21×10^{-8} rad (0.0025 arc-sec) about the Y and Z axes. The errors for the Y and Z axes are greater than those obtained for a body-point system using the same sensor implementation. The primary reasons for the degraded pointing accuracy of the IMC system relative to the body-point system with this sensor implementation is the increased sensitivity of the IMC system to position noise. This increased sensitivity probably is due to the IMC system cutoff characteristics not being as sharp as those of the body-point system investigated.

Figure 13 illustrates the image stability obtained for the derived rate sensor implementation with position noise one-quarter nominal and CMG tachometer noise one-tenth

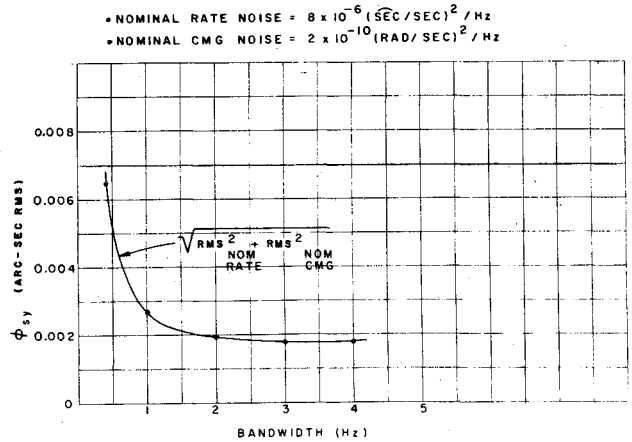

Fig. 11 Y-axis total rms pointing error resulting from noise sources: gyro hold control, CMG system.

nominal. For these conditions, minimum Y and Z axes pointing errors were obtained for a vehicle loop bandwidth of 1.25 Hz. Reduction in CMG tachometer noise was required, since the IMC system is more sensitive to this noise source than the corresponding body-point system. The reason for this increased sensitivity is that the bandwidth of the CMG system is comparatively low (between 0.05 and 0.3 Hz when considering the IMC bandwidths of 0.5 to 3 Hz). Hence, the CMG tachometer noise causes base vehicle errors that must be

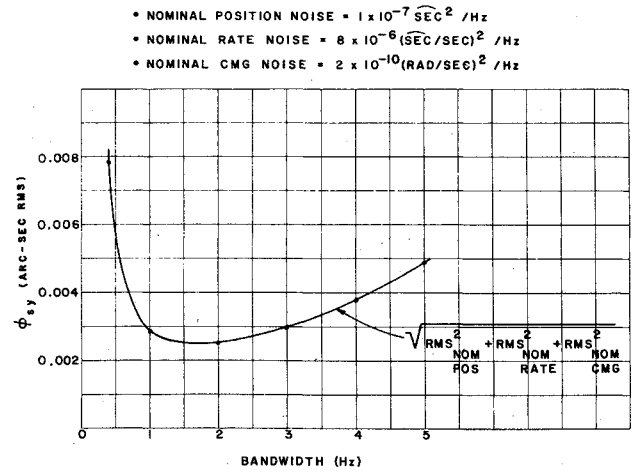

Fig. 12 *Y*-axis total rms pointing error resulting from noise sources: CMG/IMC system.

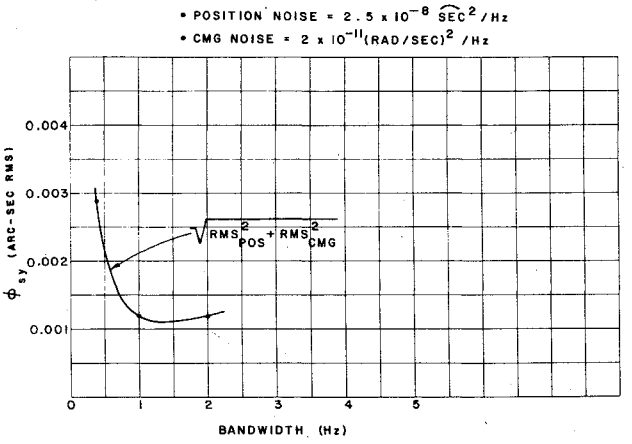

Fig. 13 *Y*-axis total rms pointing error resulting from noise sources: derived rate control, CMG/IMC system.

eliminated by the IMC system. However, the IMC system removes the image motion by secondary mirror articulation. Therefore, when the IMC system has sufficient bandwidth (0.5 to 2 Hz) to eliminate the vehicle errors due to CMG tachometer noise, the secondary mirror actually is articulating in opposition to these errors. Hence, the signal that is proportional to secondary mirror position becomes noisier as IMC system bandwidth is increased. It is this signal that is differentiated to obtain the rate signal required to drive the CMG system. This, in turn, causes excessive noise to be injected into the CMG system, resulting in the sensitivity exhibited by the IMC system for this noise source. In the body-point system, as the vehicle loop bandwidth increases to counteract the errors induced by CMG noise, the CMG's are commanded to produce an output rate, and hence torque, that is in opposition to that resulting from the CMG tachometer. Therefore, the net torque acting on the vehicle is reduced, and the position signal becomes less noisy as the loop bandwidth is increased. Hence, the body-point system is not as sensitive to CMG tachometer noise for the derived rate sensor implementation. However, the IMC system is not as sensitive to position noise as is the body-point system for the derived rate sensor implementation. This is apparent, since the differentiation of the position signal is external to the relatively high-bandwidth IMC system and is used only to drive the CMG system, which cannot respond to high-frequency noise because of its low bandwidth characteristics. The pointing performance obtained for the IMC system, for all sensor implementations studied, is shown in Table 1.

Comparison between Body-Point and IMC Systems

The image stability that can be achieved by both body-point and IMC systems is equivalent for the same magnitudes of perturbing noise sources. Both systems will meet LST pointing requirements for the amplitudes of the noise sources considered. For the derived rate sensor implementation, the body-point system is more sensitive to position noise than the equivalent IMC system, whereas the IMC system is more sensitive to CMG tachometer noise. Additional study is required to determine which system would be more desirable when considering a derived rate sensor implementation, but, for the present neither system has a clear advantage. The IMC system exhibited better stability characteristics than the body-point system in the presence of bending mode parameter variations without the use of counterbalancing. The IMC system can be made essentially independent of vehicle bending characteristics by precise counterbalancing. However, the stability margins obtained for a body-point system in the presence of realistic bending mode variations were quite adequate, and it is questionable whether the added stability potential of an IMC system is an advantage. From the point of view of system complexity, reliability, and cost, the body-point system has a distinct advantage over the equivalent IMC system. At worst, the only additional hardware required to achieve LST pointing accuracy would be three small RW's. These wheels are inexpensive, highly reliable, and represent no technical risk in their manufacture. Additionally, all investigations to date indicate that the RW's can be eliminated (especially when the vehicle is disturbed) without any appreciable penalty in pointing performance. Therefore, it is recommended that a body-point system be used for LST stabilization.

Vibrational Analysis

When considering the stringent LST pointing stability requirements, the errors caused by vibrational disturbances due to CMG wheel imbalances must be studied carefully. In order to conduct this investigation, the vibrational disturbances at the base of the CMG were estimated by computer simulation using a detailed flexible body representation of the proposed CMG. These vibrational disturbances then were applied to a complete vehicle flexible body model, and the resultant image motion was determined. The control system was not included in this analysis, since the lowest vibrational disturbance frequency was 66 Hz, well beyond the bandwidth of any proposed body-point or IMC system. The flexible body data utilized for this study assume a graphite-epoxy composition for the truss and secondary image plane, and a lock alloy composition for the solar panels. The CMG base vibrational disturbance amplitudes and the frequencies at which they occur are shown in Table 2.

These vibrational disturbances, when transmitted to the vehicle by the cluster of four single-gimbal CMG's, yielded worst-case image motion errors, as shown in Table 3 for the hard-mounted case. These errors are excessive, particularly for the vehicle *Y* axis, and indicate that the CMG's should be shock mounted if LST pointing accuracies are to be achieved in the presence of the CMG vibrational disturbance levels defined in Table 2. Similar data for the case where each CMG was placed individually on a 20-Hz, 0.707 damped shock mount also are shown in Table 3 for the shock-mounted case.

Table 2 CMG base vibrational disturbances

	66 Hz, N	133 Hz,[a] N	266 Hz, N
F_x	1.91	7.0	2.9
F_y	3.2	6.2	3.5
F_z	3.2	13.3	11.4

[a] Wheel spin frequency.

Table 3 Worst-case image motion errors due to CMG vibrational disturbances

Vehicle axis	Image motion errors	
	Hard-mounted CMG	Shock-mounted CMG
ϕ_{sx}	0.976×10^{-8} rad (0.002 arc-sec)	3.07×10^{-9} rad (0.000634 arc-sec)
ϕ_{sy}	1.7×10^{-8} rad (0.00352 arc-sec)	5.06×10^{-9} rad (0.00104 arc-sec)
ϕ_{sz}	0.884×10^{-8} rad (0.00182 arc-sec)	2.89×10^{-9} (0.000596 arc-sec)

In this case, the vibrational errors are tolerable. Thus, LST pointing accuracies can be achieved in the presence of the predicted CMG vibration levels with a 20-Hz shock mount.

In order to achieve more effective isolation from the CMG vibrational disturbances, shock mount damping should be reduced while keeping the natural frequency constant. The force transmission to the vehicle can be written as follows

$$F_{av} = \frac{\{[s/\omega_n/2\zeta)]+1\}F_a}{(s/\omega_n)^2+(2\zeta/\omega_n)s+1}$$

where ζ = shock mount damping ratio, ω_n = shock mount natural frequency, F_a = force applied to shock mount, and F_{av} = force applied to vehicle. As the shock mount damping ratio is decreased, the numerator break frequency becomes higher while the denominator break frequency remains constant. Therefore, more effective attenuation can be realized, since the falloff through the shock mount is second order between the denominator and numerator break points. Reduction of shock mount damping also is desirable from an implementation viewpoint, since materials normally have low damping. However, reduction of shock mount damping can cause stability problems when the CMG shock mount combination is inserted into the vehicle body-point control system. In addition, the CMG shock-mount combination can be unstable by itself, which is a more severe problem. Further study is required to determine the amount of shock mount damping reduction which can be tolerated.

Another area of concern when considering vibrations is the possibility of vibrational force and torque disturbances at beat frequencies, which can be within the bandpass of the CMG shock mount and hence would be transmitted directly to the vehicle without any attenuation. These beat frequencies can arise from slightly different wheel speeds of the CMG's comprising the CMG cluster. The vibrational model used in this study would not predict beats, since it did not have the required cross-feed between CMG's in the cluster, nor the CMG structural nonlinearities. Further study is needed to determine whether vibrational disturbances at beat frequencies can arise, their effect on pointing performance if they do occur, and methods that can be employed to preclude their occurrence.

Conclusions and Recommendations

The following are the major conclusions and recommendations of the study:

1) LST pointing accuracies can be met by both body-point or IMC systems, with the performance of both systems essentially equivalent. Because of the advantages of the body-point system in the areas of complexity, reliability, and cost, a body-point system is recommended for LST attitude stabilization.

2) Secondary mirror counterbalancing was not required to achieve adequate IMC system stability for the vehicle dynamic structural model considered over the range of loop bandwidths investigated.

3) LST pointing accuracies can be achieved by a body-point system consisting of four single-gimbal CMG's if friction can be modeled reasonably as a spring exhibiting saturation. However, because of the uncertainty of the actual CMG frictional characteristics, the CMG/RW system is still the recommended body-point system configuration, pending future study of CMG frictional characteristics.

4) A CMG system consisting of four single-gimbal CMG's gives the same pointing performance as the CMG/RW system when the vehicle is being torqued, for virtually any frictional description, and hence will meet LST pointing performance under this condition.

5) Of the three sensor implementations investigated for the body-point system, rate-plus-position gave best pointing performance for the nominal noise levels considered. It should be noted that rate gyro noise characteristics are uncertain, and they can be larger than the nominal values considered in this study. It therefore is possible that the pointing errors for the rate-plus-position and rate gyro hold sensor implementations can increase to where LST pointing accuracies will not be achieved. However, the noise levels required to meet LST pointing accuracies for the derived rate sensor implementation are within achievable levels. Therefore, the derived rate sensor implementation, although more sensitive to position noise, is the recommended configuration, pending further investigation of rate gyro noise characteristics.

6) The vehicle loop bandwidth should be between 1 and 2.5 Hz in order to achieve minimum vehicle pointing errors due to the various noise inputs. This applies regardless of the sensor implementation employed.

7) Projected CMG vibrational disturbances will cause excessive pointing errors unless the CMG's are shock mounted individually. A 20-HZ shock mount will yield the required vibrational isolation.

References

[1] Hartter, L.L., Rybak, S.C., Mayo, R.A., and Yeichner, J.A., "A Hard-Mounted Ultrahigh-Accuracy Pointing Control System," AIAA Paper 72-854, Aug. 14-16, 1972, Stanford, Calif.

[2] Rybak, S.C., Lieberman, S.I., Hartter, L.L., Gregory, R.L., Nakashima, A.K., and Kaczynski, R.F., "Achieving Ultrahigh-Accuracy with a Body Pointing CMG/RW Control System," AIAA Paper 73-883, Aug. 20-22, 1973, Key Biscayne, Fla.

[3] Dahl, P.R., "A Solid Friction Model," Rept. TOR-0158 (3107-18)-1, Aerospace Corporation, El Segundo, Calif., May 1968.

[4] Osborne, N.A. and Rittenhouse, D.L., "The Modeling of Friction and Its Effects on Fine Pointing Control," AIAA Paper 7H-875, Aug. 5-9, 1974, Anaheim, Calif.